Economic optimization of a Kalina cycle for a parabolic trough solar thermal power plant

Modi, Anish; Kærn, Martin Ryhl; Andreasen, Jesper Graa; Haglind, Fredrik

Published in:
Proceedings of ECOS 2015

Publication date:
2015

Document Version
Publisher's PDF, also known as Version of record

Economic optimization of a Kalina cycle for a parabolic trough solar thermal power plant

Anish Modi[a], Martin Ryhl Kærn[b], Jesper Graa Andreasen[c] and Fredrik Haglind[d]

[a] *Technical University of Denmark, DK-2800 Kgs. Lyngby, Denmark, anmod@mek.dtu.dk, CA*
[b] *Technical University of Denmark, DK-2800 Kgs. Lyngby, Denmark, pmak@mek.dtu.dk*
[c] *Technical University of Denmark, DK-2800 Kgs. Lyngby, Denmark, jgan@mek.dtu.dk*
[d] *Technical University of Denmark, DK-2800 Kgs. Lyngby, Denmark, frh@mek.dtu.dk*

Abstract:

The Kalina cycle has recently seen increased interest as a replacement for the more traditional steam Rankine cycle for geothermal, solar, ocean thermal energy conversion and waste heat recovery applications. The Kalina cycle uses a mixture of ammonia and water as the working fluid. The ammonia-water mixture evaporates and condenses with a temperature glide, thus providing a better match with the heat source/sink temperature profile. This better match results in reduced thermal irreversibility, but at the cost of relatively larger heat exchanger areas. The parabolic trough collector is the most mature technology for the conversion of solar thermal energy into electricity. In this paper, a Kalina cycle and a steam Rankine cycle are compared in terms of the total capital investment cost for use in a parabolic trough solar thermal power plant without storage. In order to minimize the total capital investment cost of the Kalina cycle power plant (the solar field plus the power cycle), an optimization was performed by varying the turbine outlet pressure, the separator inlet temperature and the separator inlet ammonia mass fraction. All the heat exchangers were modelled as shell and tube type using suitable heat transfer correlations, and appropriate cost functions were used to estimate the costs for the various plant components. The optimal capital investment costs were determined for several values of the turbine inlet ammonia mass fraction and among the compared cases, the Kalina cycle has the minimum capital investment cost of 5851.2 United States Dollars (USD) per kW of net electrical power output. The steam Rankine cycle has much higher investment costs (7625.1 USD/kW) mainly due to the limitation imposed by the minimum turbine outlet vapour quality constraint.

Keywords:
Economic optimization, heat exchanger, Kalina cycle, parabolic trough, solar thermal power plant.

1. Introduction

Solar thermal power plants (STPPs) are expected to play an important role in the future energy mix [1]. An STPP consists of mainly three sections: the solar field, the storage system and the power cycle. The STPPs can be operated with either a multi-fluid configuration where the heat transfer fluid in the receiver is different from the power cycle working fluid, or with a direct vapour generation configuration where pressurized vapour is generated directly in the receiver and transported to the turbine. Parabolic trough solar collectors have been by far the commercially most successful collector systems, currently with majority of the world's commercial STPPs operating with this technology. However, there is a limitation to using the parabolic trough collectors. The achievable solar field outlet temperature is restricted by the thermal stability of the heat transfer fluid such as Therminol VP-1 which cannot be used above 400 °C [2]. This significantly limits the overall solar-to-electric efficiency for the plant. One way to improve this efficiency is to use advanced power cycles such as the Kalina cycle [3]. The Kalina cycle uses a mixture of ammonia and water as the cycle working fluid. The exergy losses during a heat transfer process can be reduced by using a suitable zeotropic working fluid, which can evaporate and condense with a temperature glide, contrary to the constant evaporating and condensing temperature for a pure substance [4]. The temperature glide makes it possible to have a better match with the heat

source/sink temperature profile. The reduction in the irreversibility comes at the cost of relatively larger heat exchanger areas, and the use of a more complex cycle layout, thus possibly resulting in increased capital investment.

There were proposals to incorporate the Kalina cycle for waste heat recovery plants, geothermal power plants and solar power plants, with low or medium range temperatures at the turbine inlet. Bombarda et al. [5] presented a thermodynamic comparison between the Kalina cycle and an organic Rankine cycle (ORC) for heat recovery from diesel engines. They concluded that although the obtained electrical power outputs are nearly equal, the Kalina cycle requires a much higher turbine inlet pressure to attain the same, thereby making it unjustified for such use. Singh and Kaushik [6] presented energy and exergy analysis and optimization of a Kalina cycle coupled with a coal-fired steam power plant for exhaust heat recovery. They found out that at a turbine inlet pressure of 40 bar, an ammonia mass fraction of 0.8 gives the maximum cycle efficiency and the highest exergy destruction occurs in the evaporator. Campos Rodríguez et al. [7] presented an exergetic and economic comparison between a Kalina cycle and an ORC for a low temperature geothermal power plant. They found that the Kalina cycle produces 18 % more power than the ORC with 37 % less mass flow rate. In addition, the Kalina cycle had 17.8 % lower levelized electricity costs than the ORC. Wang et al. [8] presented a parametric analysis and optimization of a Kalina cycle driven by solar energy. They found that the net power output and the system efficiency are less sensitive to the turbine inlet temperature under given conditions and that there exists an optimal turbine inlet pressure which results in maximum net power output. Coskun et al. [9] presented a comparison between different power cycles for a medium temperature geothermal resource. They found that the Kalina cycle and the double flash cycle provided the least levelized cost of electricity and hence the lowest payback periods.

With regards to using the Kalina cycle with high turbine inlet temperatures, Ibrahim and Kovach [10] studied the effect of varying the ammonia mass fraction and the separator temperature on the cycle efficiency for a Kalina bottoming cycle using gas turbine exhaust as the heat source. The Kalina cycle turbine inlet conditions were 482 °C and 59.6 bar. The authors found that the Kalina cycle is 10-20 % more efficient than the Rankine cycle with the same boundary conditions. Nag and Gupta [11] performed an exergy analysis of a Kalina cycle with gas turbine exhaust as the heat source for turbine inlet temperature between 475 °C and 525 °C, and a turbine inlet pressure of 100 bar. They concluded that the important parameters affecting the cycle efficiency are the turbine inlet temperature, composition and the separator temperature. Dejfors et al. [12] presented an analysis of using ammonia-water power cycles for direct fired cogeneration plants with a maximum temperature of 540 °C. They concluded that for a cogeneration configuration, the Rankine cycle performs better than the Kalina cycle whereas for the conventional condensing power application, the performance of the Kalina cycle is better. Knudsen et al. [13] presented the results from the simulation and exergy analysis of a Kalina cycle for an STPP having a turbine inlet temperature of 550 °C when the heat input is from a solar receiver, and 480 °C when the heat input is from a molten-salt storage system. The authors varied the heat input to the cycle so as to maintain the turbine inlet conditions, while assuming the same mass flow rate for all the cases. Modi et al. [14] presented a comparison between a Rankine cycle and an ammonia-water cycle for STPPs with a turbine inlet temperature of 450 °C. The cycle energy efficiency and the storage size requirement were used as the comparison parameters. Modi and Haglind presented the exergy analysis of a particular Kalina cycle layout [15] and thermodynamic optimization of four Kalina cycle layouts [16] for central receiver STPPs with direct steam generation.

The purpose of this paper is to optimize the Kalina cycle for a parabolic trough STPP (without storage) for minimum total capital investment costs, and compare the economic performance of the Kalina cycle with that of the standard steam Rankine cycle. The comparison is made in terms of the total capital investment per kW of net electrical power output, and for different turbine inlet

ammonia mass fractions. A detailed modelling approach was used for the estimation of the heat exchanger area with the zeotropic ammonia-water mixtures as the working fluid. This approach is more advanced as compared with the previous economic studies such as those presented in [17,18] which assume a constant overall heat transfer coefficient to estimate the heat exchanger areas. In the paper, Section 2 presents the assumptions and the modelling procedure; Section 3 presents the results from the Kalina cycle optimization, discussions of the results and comparison with the steam Rankine cycle; and Section 4 concludes the paper.

2. Methods

Several cycle layouts have been proposed for power plants operating with a Kalina cycle with input from different types of heat sources [19]. In this study, the layout was kept in a simple form with one separator and two recuperators (termed as KC12 in [16]) as it was compared with the most basic steam Rankine cycle. For the Kalina cycle (Fig. 1), the working solution ammonia-water mixture (stream 1) is expanded in the turbine TUR which is connected to the electrical generator GEN. Energy is recovered from stream 2 to preheat the working solution in the recuperator RE1. In order to have a low condensation pressure in the condenser CD1, a separator SEP is used from which a rich ammonia vapour (stream 11) and a lean ammonia liquid (stream 12) are obtained. The lean liquid is mixed with the working solution (in the mixer MX1) and thus the ammonia mass fraction in the condenser CD1 is reduced. A throttle valve is used to bring the pressure of the lean liquid (stream 12) down to the pressure level of the working fluid (stream 4) before mixing in the mixer MX1. The rich vapour (stream 11) is mixed with the basic solution (stream 8) to form the working fluid (stream 14) before going through the condenser CD2 and then the pump PU2. After the recuperator RE1, the working fluid (stream 17) is heated up to the turbine inlet temperature in the boiler consisting of an economizer (EC), an evaporator (EV) and a superheater (SH).

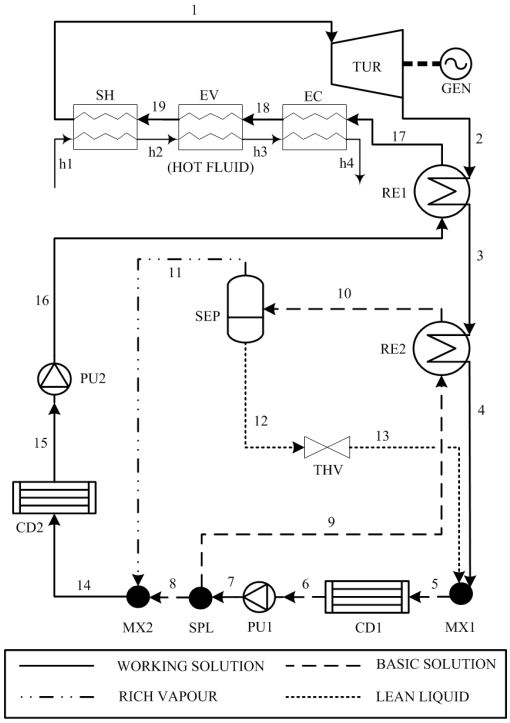

Fig. 1. Layout of the Kalina cycle KC12.

The steam Rankine cycle considered in this study was a typical four-component cycle including a steam turbine, a wet-cooled condenser, a pump, and a boiler similar to the one shown in Fig.1.

The following assumptions were made for the cycle optimization. Both the cycles were modelled in steady state. The hot fluid (Therminol VP-1 [2]) temperature at the boiler inlet (T_{h1}) was assumed to be 390 °C. The minimum temperature of the hot fluid was fixed at 120 °C so as to avoid rapid variation of the thermophysical properties in the operating temperature range, e.g. the viscosity of the fluid decreases very quickly below this temperature [2]. The turbine inlet temperature and pressure were fixed at 370 °C and 100 bar. The isentropic efficiencies of the turbine and the pumps were 85 % and 70 % respectively. The turbine mechanical efficiency and the generator efficiency were both 98 %. The plant was designed for a net electrical power output of 20 MW. The minimum allowed vapour quality at the turbine outlet was 90 %. The condenser cooling water inlet and outlet temperatures were fixed at 20 °C and 30 °C respectively. The boiler had an approach temperature of 20 °C and a minimum pinch point temperature difference (PPTD) of 15 °C. The recuperators and the condensers had a minimum PPTD of 8 °C and 4 °C respectively. For the Kalina cycle, the minimum separator inlet vapour quality was fixed at 5 %, while pressure drops and heat losses were neglected for both the cycles.

For the Kalina cycle optimization, the objective was to minimize the total capital investment cost of the power plant (the solar field plus the power cycle). The decision variables were the turbine outlet pressure, the separator inlet temperature and the separator inlet ammonia mass fraction. The optimization was performed as follows. The design parameters were provided as input to the genetic algorithm. These included the turbine inlet temperature, pressure and ammonia mass fraction, the generator power output, the efficiencies of the turbine, pumps and generator, etc. The lower and upper bounds for the decision variables were also provided as input. The genetic algorithm then selected an initial population covering the entire search space and began the optimization process, moving gradually towards the optimum solution. In case there was an error in the calculation of the thermodynamic properties by REFPROP, or the mass or energy balances were not satisfied with a residual below or equal to 0.001 %, the solution was rejected. The initial population for the genetic algorithm was 50, the maximum number of generations was 30, the elite count was 2, the crossover fraction was 0.8 and the function tolerance was 10^{-6}. The simulations were run using MATLAB (R2015a) [20], and the optimization was performed using the genetic algorithm from the Optimization Toolbox. The thermodynamic properties of both pure water for the steam Rankine cycle and the ammonia-water mixtures for the Kalina cycle were calculated using the REFPROP (9.1) interface for MATLAB [21]. The default property calculation method for the ammonia water mixtures in REFPROP is using the Tillner-Roth and Friend formulation [22]. However, this formulation is highly unstable and fails to converge on several occasions, especially in the two phase regions, near critical point and at higher ammonia mass fractions. Therefore, an alternative formulation called ‘Ammonia (Lemmon)’ was tested and used. It was found to be more stable and with fewer convergence failures [16].

The detailed methodology of solving the high temperature Kalina cycle was presented in [16] by the authors. For the Kalina cycle parametric study, the turbine inlet ammonia mass fraction was varied between 0.5 and 0.8. The overall approach for Kalina cycle optimization in the current study is as follows:

1. Solve the cycle thermodynamically with the methodology presented in [16].
2. Obtain temperature profiles for the heat exchangers and the thermodynamic state for the cycle.
3. Allocate the hot and cold fluids on the shell or tube sides.
4. Estimate the heat exchanger area using appropriate heat transfer correlations.
5. Estimate the heat exchanger costs using the area as input, and the costs of other equipment using suitable cost functions.
6. Update the above costs to the reference time (January 2014) using the Marshall and Swift Equipment Cost Index [23].

7. Run genetic algorithm until the total plant capital cost per kW of net electrical power output is minimized.

The steam Rankine cycle was solved directly using mass and energy balances to find out the operating states which provide the minimum condenser pressure while satisfying the design constraints such as the turbine outlet vapour quality and the minimum PPTD. The performance of the components in the steam Rankine cycle were assumed equal to the corresponding components in the Kalina cycle.

2.1. Heat exchanger model

All the heat exchangers were modelled as shell-and-tube type using the Bell-Delaware method assuming counter-flow arrangement. For simplicity, the heat exchangers were always assumed to have a single shell pass and a single tube pass. Since the temperature profiles in the heat exchangers were not always linear, the heat exchangers were divided into 50 control volumes (CVs), and the area for each CV was calculated. The area of the heat exchanger would then be the sum of the areas of all the CVs. Table 1 shows an overview of the heat transfer correlations used in this study. A detailed assessment of various transport property estimation methods (for thermal conductivity and viscosity) for ammonia-water mixtures is provided in [24]. The ammonia-water mixture transport properties were calculated using the methods by El-Sayed [25] as presented in [26]. The transport properties for water for the steam Rankine cycle were obtained from REFPROP.

Table 1. Heat transfer correlations used in this study

Description	Correlation	Reference
Single phase in-tube flow, mixture and pure fluid	Gnielinski (1976)	[27]
Condensing in-tube flow, mixture	Shah (2013) with Silver-Bell-Ghaly (1972) correction	[28,29]
Condensing in-tube flow, pure fluid	Shah (1979)	[30]
Evaporating in-tube flow, mixture and pure fluid	Shah (1982)	[31]
Single phase flow, shell side, mixture and pure fluid	Smith (2005)	[32]
Condensing flow, shell side, mixture	Kern (1950) as presented in Smith (2005) with Silver-Bell-Ghaly (1972) correction	[29,32,33]

In order to allocate the shell side and the tube side to the fluids [32,34], the fluid with higher pressure was always allocated on the tube side; and wherever possible, the two-phase flow would be allocated the tube side. In case there was a two-phase to two-phase heat transfer, the evaporating fluid was put in the tubes while the condensing fluid was allocated the shell side. The following assumptions were made with regards to the heat exchanger geometry [32,34,35]: the maximum shell and tube side liquid velocities were 0.8 m/s and 2 m/s [34] to avoid excessive pressure drops; the maximum vapour velocity on both the shell and tube sides was 22 m/s [11] for the low and intermediate pressure heat exchangers (recuperator RE2 and both the condensers), and was 10 m/s [34] for the high pressure heat exchangers (recuperator RE1 and the boiler); the tube outer diameter was 20 mm, and the thickness was 1.6 mm for the low and intermediate pressure heat exchangers and 2.6 mm for the high pressure heat exchangers, two of the common standard tube sizes [34]; the 45 degrees square pattern was assumed for the tube arrangement to maximize the heat transfer; the tube pitch to tube outer diameter ratio was maintained between 1.25 and 1.5; a baffle cut of 25 % was fixed; and the effect of the ratio of the bulk fluid viscosity to the wall fluid viscosity was neglected during the heat transfer calculations, except in case of the boiler with thermal oil on the shell side. The overall heat exchanger area calculation approach used in this study was similar to the one presented in [24].

2.2. Solar field model

The aim here was to estimate the required solar field and land areas at the power cycle design point:

$$A_{\mathrm{SF}} = SM \cdot \frac{\dot{Q}_{\mathrm{HTF}}}{\left[ANI \cdot \eta_{\mathrm{opt}} \cdot IAM - U_{\mathrm{loss}} \cdot \left(T_{\mathrm{av}} - T_{\mathrm{amb}} \right) \right]} \tag{1}$$

$$\dot{Q}_{\mathrm{HTF}} = \dot{m}_{17} \cdot \left(h_1 - h_{17} \right) = \dot{m}_{\mathrm{oil}} \cdot \left(h_{\mathrm{h1}} - h_{\mathrm{h4}} \right) \tag{2}$$

$$ANI = DNI \cdot \cos\theta \tag{3}$$

$$IAM = 1 - 2.23073 \times 10^{-4} \cdot \theta - 1.1 \times 10^{-4} \cdot \theta^2 + 3.18596 \times 10^{-6} \cdot \theta^3 - 4.85509 \times 10^{-8} \cdot \theta^4 \tag{4}$$

$$\eta_{\mathrm{opt}} = \rho_{pt} \cdot \alpha_{pt} \cdot \tau_{pt} \cdot \gamma_{pt} \cdot F_e \tag{5}$$

$$T_{\mathrm{av}} = \frac{T_{\mathrm{h1}} + T_{\mathrm{h4}}}{2} \tag{6}$$

$$\theta = \cos^{-1}\left(\sqrt{\cos^2\theta_z + \cos^2\delta \cdot \sin^2\omega} \right) \tag{7}$$

$$\theta_z = \cos^{-1}\left(\cos\phi \cdot \cos\delta \cdot \cos\omega + \sin\phi \cdot \sin\delta \right) \tag{8}$$

$$\omega = 15 \cdot \left(t_{\mathrm{s}} - 12 \right) \tag{9}$$

$$t_{\mathrm{s}} = t_{\mathrm{clk}} + \frac{\psi_{\mathrm{std}} - \psi}{15} + \frac{EOT}{60} - DST \tag{10}$$

$$EOT = 229.2 \cdot \begin{pmatrix} 0.000075 + 0.001868 \cdot \cos B - 0.032077 \cdot \sin B - \\ 0.014615 \cdot \cos 2B - 0.04089 \cdot \sin 2B \end{pmatrix} \tag{11}$$

$$\delta = \frac{180}{\pi} \cdot \begin{pmatrix} 0.006918 - 0.399912 \cdot \cos B + 0.070257 \cdot \sin B - 0.006758 \cdot \cos 2B + \\ 0.000907 \cdot \sin 2B - 0.002697 \cdot \cos 3B + 0.00148 \cdot \sin 3B \end{pmatrix} \tag{12}$$

$$B = \frac{360}{365} \cdot \left(n - 1 \right) \tag{13}$$

The total land area required (A_{LAND}) was assumed to be 2.4 times the solar field aperture area (A_{SF}) [36]. In the above equations, *ANI* is the aperture normal irradiance for the design *DNI* value of 800 W/m^2. The solar multiple (*SM*) was assumed to be 1.3 [37], the overall heat loss coefficient (U_{loss}) to be 0.1 W/(m^2 K) [38], and the ambient temperature (T_{amb}) to be 25 °C. The solar field average temperature (T_{avg}) was calculated as the average of the solar field inlet and outlet temperatures. As suggested in [37], the solar field was designed for June 21 (n = 172 in (13)) at 12 noon local clock time (t_{clk} = 12 in (10)). The parabolic trough was assumed to be LS3 [37] for calculation of the incidence angle modifier *IAM* using (4). The incidence angle θ was calculated in (7) assuming North-south orientation with East-West tracking [39]. The zenith angle θ_z was calculated using (8) with the latitude (ϕ), declination angle (δ) and hour angle (ω) as the input. The power plant was assumed to be located in Seville, Spain (coordinates 37.25° N, 5.54° W), thus the latitude ϕ becomes 37.25 degrees. The declination angle is calculated using (12) as suggested in

[39]. The hour angle is calculated using the local solar time t_s. The local solar time is a function of the local clock time, the site latitude (ψ), the standard meridian for the site (ψ_{std}) which is 15° E for Seville Spain, the equation of time (*EOT*) calculated using (11) as presented in [39], and the daylight savings time (*DST*) which is equal to one when it is applicable, otherwise zero. For the calculations, West was taken as the positive direction, and all the angles were in degrees.

2.3. Cost calculations

The total plant capital investment cost was calculated using:

$$C_{TOT} = C_{PC} + C_{SF} + C_{LAND} + C_{CNT} \quad (14)$$

$$C_{CNT} = 0.2 \cdot \left(C_{PC} + C_{SF} + C_{LAND}\right) \quad (15)$$

$$C_{PC} = C_{TUR} + C_{GEN} + \sum C_{PU} + \sum C_{RE} + \sum C_{CD} + C_{BLR} + C_{SEP} + C_{MISC} \quad (16)$$

$$C_{SF} = 206 \cdot 1.3 \cdot A_{SF} \quad (17)$$

$$C_{LAND} = 2 \cdot 1.3 \cdot A_{LAND} = 2 \cdot 1.3 \cdot \left(2.4 \cdot A_{SF}\right) \quad (18)$$

$$C_{SEP} = F_p \cdot 10^{k1 + k2 \cdot log(H) + k3 \cdot (log(H))^2} \quad (19)$$

The cost functions for the turbine (C_{TUR}), the pumps (C_{PU}), the generator (C_{GEN}) and the heat exchangers (C_{RE}, C_{CD} and C_{BLR} (C_{SH}+C_{EV}+C_{EC})) are given in [40]. The miscellaneous cost (C_{MISC}) includes the cost for installation, piping, instrumentation and control, and electrical equipment and material, in total it is 1.31 times the purchased equipment cost for the power cycle [41]. The cost of the heat exchangers was updated using a pressure and a temperature factor as suggested in [32]. The solar field cost (C_{SF}) and the total land cost (C_{LAND}) were calculated using the rates given in [42]. The rates were multiplied by a factor of 1.3 to convert them from Euros to United States Dollars (USDs). All the cost functions provide output in USDs. The surcharge for construction, engineering and contingencies was assumed to be 20 % of the sum of the cost of the power cycle, the solar field and the land as suggested in [42]. The cost of the separator (C_{SEP}) was calculated using (19) as suggested in [43]. In (19), the pressure factor F_p was calculated as described in [43], and the height (*H*) was calculated using the volume flow rate to the separator, the residence time assumption of 3 min, and a height to diameter ratio of 3 which is common in commercial applications [44].

3. Results and discussion

The total investment cost of the plant per kW of net electrical power output and other key results from the Kalina cycle optimization are shown in Table 2.

Table 2. Optimization results for the Kalina cycle for 100 bar turbine inlet pressure

Turbine inlet ammonia mass fraction	Working solution (stream 1) mass flow rate (kg/s)	Separator inlet temperature T_{10} (°C)	Turbine outlet pressure p_2 (bar)	Total investment cost per kW of net electrical power output (USD/kW)
0.5	31.4	70.3	1.43	5851.2
0.6	33.7	82.9	2.23	6009.7
0.7	37.6	53.7	3.87	6159.0
0.8	43.0	47.5	6.76	6070.4

For the Rankine cycle, the total plant capital investment cost was 7625.1 USD/kW. Fig. 2 shows the capital cost breakdown for the steam Rankine cycle ('SRC' in the figure) and the Kalina cycle for different turbine inlet ammonia mass fractions (0.5 to 0.8). The costs shown are only for power cycle equipment, i.e. not including the solar field, land and other costs.

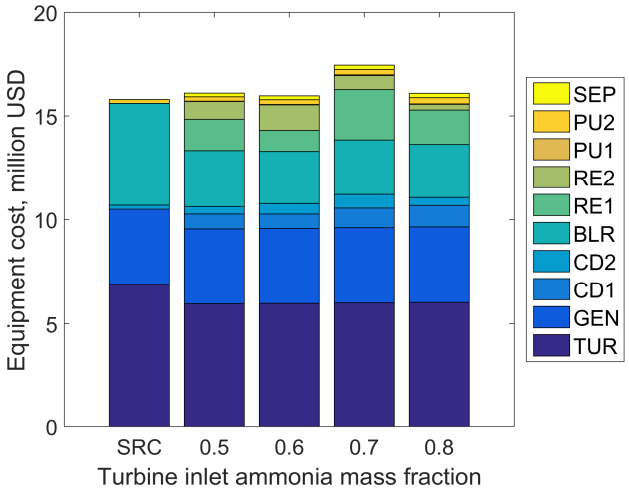

Fig. 2. Equipment cost for the Kalina and the steam Rankine power cycles.

As may be observed from Fig. 2 for the Kalina cycle, the investment cost for the condenser CD1 first decreases slightly, then increases, while that for the condenser CD2 first increases, and then decreases with the increasing turbine inlet ammonia mass fraction. For both the condensers, the respective cost trend is observed because of the increase or decrease in the heat transferred in the condenser for the optimal solution. The cost of the recuperator RE2 first increases, then decreases, while for the recuperator RE1, the cost first decreases, then increases and finally decreases again with increasing turbine inlet ammonia mass fraction. This is mainly because a limit on the PPTD was only applied to the minimum value, while the PPTD for the recuperator RE1 took a very high value for the 0.6 turbine inlet ammonia mass fraction in order to achieve the minimum plant cost, thereby reducing the recuperator RE1 cost significantly for this case. In future studies, a limit on the maximum possible pinch point temperature difference will also be imposed so as to curtail this exceptional behaviour. The cost of the pump PU1 is small compared with the cost of the pump PU2 and the separator SEP. The cost of the pump PU2 exhibits an increasing trend with increasing turbine inlet ammonia mass fraction. This is because of the increased mass flow rate for the optimal solutions with increasing value of the turbine inlet ammonia mass fractions. The separator costs are also increasing with the increasing ammonia mass fraction, mainly because of the increasing condensation pressure for the condenser CD2, which is the same as the separator pressure.

It should be noted that the optimal solution for the economic optimization is not the same as the optimal solution for a thermodynamic optimization [16]. The economic optimal solution does not correspond to the maximum design cycle efficiency solution, and therefore it is difficult to directly relate the cost trend with that of the thermodynamic trend. In the economically optimal solutions, the solar field is about half the total plant cost. In the scenario where the solar field cost would constitute the majority of the total plant cost, the total cost will be highly sensitive to the cycle efficiency. This is because for a fixed net electrical power output, the plant with a higher efficiency will require a lower heat input in the boiler, thus requiring a smaller solar field.

The much higher investment cost for the steam Rankine cycle is primarily due to the minimum vapour quality constraint at the turbine outlet (7625.1 USD/kW for a minimum turbine outlet vapour quality of 90 %). This constraint significantly increases the condensation pressure, and

makes the cycle very inefficient, thereby also increasing the solar field size. This issue can be resolved by including reheat (which is common practice in steam Rankine cycles). The addition of reheat however increases the complexity of the power cycle, and thus also the cost. Even when the turbine outlet minimum vapour quality requirement is reduced from 90 % to 85 %, the Rankine cycle cost at 6104.9 USD/kW still remains higher than the Kalina cycle costs for three of the four compared cases. The above results suggest that there is a potential benefit in using the Kalina cycle for a parabolic trough STPP without storage. More rigorous thermodynamic and economic models are however required for further analysis. For instance, the assumption of neglecting the pressure losses in the cycle favours the Kalina cycle as it has more components. Similarly, a relatively complex Kalina cycle is compared with a simple four component steam Rankine cycle, and having a more advanced layout could make the Rankine cycle more competitive. Finally, addition of economic parameters (e.g. operations and maintenance costs, interest rates, etc.) over the life of the power plant will enable calculating the levelized cost of electricity for the power plant, and compare the performance of the different power cycles more thoroughly. Consideration of part-load performance is important for a solar power plant, and a full thermoeconomic analysis is necessary before deriving any concrete conclusions. These will be the topics for future studies.

4. Conclusion

A Kalina cycle with two recuperators and two condensers for use with a parabolic trough STPP without storage was modelled and optimized for minimum capital investment cost. The total plant cost included the cost of the solar field, the power cycle, the required land area and contingencies. The results suggest that at a turbine inlet pressure of 100 bar, the Kalina cycle results in the minimum cost at 5851.2 USD/kW among the compared cases. The Kalina power cycle capital investment cost first decreases, then increases and finally decreases with increasing turbine inlet ammonia mass fraction, while the total plant costs with the Kalina cycle first increases, then decreases. When compared with a simple steam Rankine cycle for the same application, the Kalina cycle shows better economic value in terms of lower capital investment costs. The major portion of the total cost belongs to the solar field. The Rankine cycle efficiency is limited by a huge extent because of the minimum turbine outlet vapour quality constraint. Even when this limit is relaxed, the Kalina cycle still showed better performance for three out the four compared turbine inlet ammonia mass fractions. However, more rigorous thermodynamic and economic models are required for a more thorough comparison between the two cycles for solar applications.

Nomenclature

A	area, m^2
C	cost, USD
C_p	isobaric specific heat capacity, J/(kg K)
DST	daylight savings time, h
EOT	equation of time, min
F_e	soiling factor
F_p	pressure factor for cost calculation
h	specific enthalpy, J/kg
H	height, m
$\dot{m}$	mass flow rate, kg/s
p	pressure, bar
Q	heat rate, W
SM	solar multiple
t	time, h

T temperature, °C or K

U_{loss} overall heat loss coefficient for the solar field, W/(m^2 K)

Greek symbols

α_{pt} receiver absorptivity

γ_{pt} intercept factor

δ declination angle, degrees

η efficiency

θ incidence angle, degrees

θ_z zenith angle, degrees

ρ_{pt} parabolic trough mirror reflectivity

τ_{pt} receiver tube glass cover transmissivity

ϕ latitude, degrees North

ψ longitude, degrees West

ω hour angle, degrees

Subscripts and components

amb ambient

av average

BLR boiler

CD condenser

clk local clock time

CNT construction, engineering and contingencies

EC economizer

EV evaporator

GEN generator

HTF heat transfer fluid

LAND land requirement

MISC miscellaneous cost for the power cycle

MX mixer

opt optical

PC power cycle

PU pump

RE recuperator

s local solar time

SEP separator

SF solar field

SH superheater

SPL splitter

std standard longitude/meridian

TOT total

TUR turbine

References

[1] Greenpeace International, SolarPACES, and ESTELA, 2009, Concentrating Solar Power: Global Outlook 2009, Amsterdam, Netherlands.

[2] SOLUTIA, 2015, "Therminol VP-1" [Online]. Available: www.twt.mpei.ac.ru/TTHB/HEDH/HTF-VP1.PDF. [Accessed: 22-Feb-2014].

[3] Kalina A. I., 1984, "Combined-cycle system with novel bottoming cycle," J. Eng. Gas Turbines Power, **106**, pp. 737–742.

[4] Angelino G., and Colonna Di Paliano P., 1998, "Multicomponent working fluids for organic Rankine cycles (ORCs)," Energy, **23**(6), pp. 449–463.

[5] Bombarda P., Invernizzi C. M., and Pietra C., 2010, "Heat recovery from diesel engines: A thermodynamic comparison between Kalina and ORC cycles," Appl. Therm. Eng., **30**(2-3), pp. 212–219.

[6] Singh O. K., and Kaushik S. C., 2013, "Energy and exergy analysis and optimization of Kalina cycle coupled with a coal fired steam power plant," Appl. Therm. Eng., **51**(1-2), pp. 787–800.

[7] Campos Rodríguez C. E., Escobar Palacio J. C., Venturini O. J., Silva Lora E. E., Cobas V. M., Marques dos Santos D., Lofrano Dotto F. R., and Gialluca V., 2013, "Exergetic and economic comparison of ORC and Kalina cycle for low temperature enhanced geothermal system in Brazil," Appl. Therm. Eng., **52**(1), pp. 109–119.

[8] Wang J., Yan Z., Zhou E., and Dai Y., 2013, "Parametric analysis and optimization of a Kalina cycle driven by solar energy," Appl. Therm. Eng., **50**(1), pp. 408–415.

[9] Coskun A., Bolatturk A., and Kanoglu M., 2014, "Thermodynamic and economic analysis and optimization of power cycles for a medium temperature geothermal resource," Energy Convers. Manag., **78**, pp. 39–49.

[10] Ibrahim M. B., and Kovach R. M., 1993, "A Kalina cycle application for power generation," Energy, **18**(9), pp. 961–969.

[11] Nag P. K., and Gupta A. V. S. S. K. S., 1998, "Exergy analysis of the Kalina cycle," Appl. Therm. Eng., **18**(6), pp. 427–439.

[12] Dejfors C., Thorin E., and Svedberg G., 1998, "Ammonia-water power cycles for direct-fired cogeneration applications," Energy Convers. Manag., **39**(16-18), pp. 1675–1681.

[13] Knudsen T., Clausen L. R., Haglind F., and Modi A., 2014, "Energy and exergy analysis of the Kalina cycle for use in concentrated solar power plants with direct steam generation," Energy Procedia, **57**, pp. 361–370.

[14] Modi A., Knudsen T., Haglind F., and Clausen L. R., 2014, "Feasibility of using ammonia-water mixture in high temperature concentrated solar power plants with direct vapour generation," Energy Procedia, **57**, pp. 391–400.

[15] Modi A., and Haglind F., 2014, "Performance analysis of a Kalina cycle for a central receiver solar thermal power plant with direct steam generation," Appl. Therm. Eng., **65**(1-2), pp. 201–208.

[16] Modi A., and Haglind F., 2015, "Thermodynamic optimisation and analysis of four Kalina cycle layouts for high temperature applications," Appl. Therm. Eng., **76**, pp. 196–205.

[17] Dorj P., 2005, "Thermoeconomic analysis of a new geothermal utilization CHP plant in Tsetserleg, Mongolia," The United Nations University.

[18] Larsen U., Nguyen T.-V., Knudsen T., and Haglind F., 2014, "System analysis and optimisation of a Kalina split-cycle for waste heat recovery on large marine diesel engines," Energy, **64**, pp. 484–494.

[19] Zhang X., He M., and Zhang Y., 2012, "A review of research on the Kalina cycle," Renew. Sustain. Energy Rev., **16**(7), pp. 5309–5318.

[20] MathWorks, 2015, "MATLAB" [Online]. Available: www.mathworks.se/products/matlab. [Accessed: 16-Mar-2015].

[21] National Institute for Standards and Technology, 2015, "REFPROP MATLAB Interface" [Online]. Available: www.boulder.nist.gov/div838/theory/refprop/LINKING/Linking.htm#MatLabApplications. [Accessed: 08-Apr-2015].
[22] Tillner-Roth R., and Friend D. G., 1998, "A Helmholtz free energy formulation of the thermodynamic properties of the mixture {water+ammonia}," J. Phys. Chem. Ref. Data, **27**(1), pp. 63–96.
[23] Marshall Valuation Services, 2014, "Comparative cost indexes," (January).
[24] Kærn M. R., Modi A., Jensen J. K., and Haglind F., 2015, "An assessment of transport property estimation methods for ammonia-water mixtures and their influence on heat exchanger size," Int. J. Thermophys.
[25] El-Sayed Y., 1988, "On exergy and surface requirements for heat transfer processes involving binary mixtures," The Winter Annual Meeting of the American Society of Mechanical Engineers, ASME, Chicago, Illinois, USA, pp. 19–24.
[26] Thorin E., 2001, "Thermophysical properties of ammonia-water mixtures for prediction of heat transfer areas in power cycles," Int. J. Thermophys., **22**(1), pp. 201–213.
[27] Bergman T. L., Lavine A. S., Incropera F. P., and Dewitt D. P., 2011, Fundamentals of heat and mass transfer, John Wiley & Sons, Inc., Jefferson City, USA.
[28] Shah M. M., Mahmoud A. M., and Lee J., 2013, "An assessment of some predictive methods for in-tube condensation heat transfer of refrigerant mixtures," ASHRAE Trans., **119**(2), pp. 38–51.
[29] Bell K. J., and Ghaly M. A., 1972, "An approximate generalized design method for multicomponent/partial condensers," 13th National Heat Transfer Conference, AIChE-ASME, Denver, Colorado, USA.
[30] Shah M. M., 1979, "A general correlation for heat transfer during film condensation inside pipes," Int. J. Heat Mass Transf., **22**, pp. 547–556.
[31] Shah M. M., 1982, "Chart correlation for saturated boiling heat transfer: equations and further study," ASHRAE Trans., **88**(1), pp. 185–196.
[32] Smith R., 2005, Chemical Process - Design and Integration, John Wiley & Sons, Ltd., West Sussex.
[33] Kern D. Q., 1950, Process Heat Transfer, McGraw-Hill Book Company, Singapore.
[34] Sinnott R. K., 2005, Coulson & Richardson's Chemical Engineering Volume 6, Elsevier Butterworth-Heinemann, Oxford, UK.
[35] Nag P. K., 2008, Power plant engineering, Tata Mc-Graw Hill Publishing Company Limited, New Delhi, India.
[36] NREL, 2015, "System Advisor Model."
[37] Lovegrove K., and Stein W., eds., 2012, Concentrating solar power technology: Principles, Developments and Applications, Woodhead Publishing Limited, Cambridge, UK.
[38] Desai N. B., and Bandyopadhyay S., 2015, "Optimization of concentrating solar thermal power plant based on parabolic trough collector," J. Clean. Prod., **89**, pp. 262–271.
[39] Duffie J. A., and Beckman W. A., 2006, Solar Engineering of Thermal Processes, John Wiley & Sons, Inc., Hoboken, New Jersey, USA.
[40] Modi A., and Haglind F., 2014, "Optimisation of a Kalina cycle for a central receiver solar thermal power plant," World Renewable Energy Congress XIII, WREN, London, UK.
[41] Bejan A., Tsatsaronis G., and Moran M., 1996, Thermal Design & Optimization, John Wiley & Sons, Inc.
[42] Pitz-Paal R., Dersch J., and Milow B., 2005, ECOSTAR European Concentrated Solar Thermal Road-Mapping.
[43] Ulrich G. D., 1984, A Guide to Chemical Engineering Process Design and Economics, John Wiley & Sons, Inc., New Jersey, USA.
[44] The Alstrom Corporation, 2015, "Two-phase flow separators" [Online]. Available: www.alstromcorp.com/PDFCatalogue/SECTION 5/ALMUS.pdf. [Accessed: 26-Feb-2015].